
**Pacific Northwest
National Laboratory**

Operated by Battelle for the
U.S. Department of Energy

RECEIVED

JAN 31 2000

OSTI

**Analysis of Several Hazardous
Conditions for Large Transfer and
Back-Dilution Sequences in
Tank 241-SY-101**

CW Stewart
LA Mahoney
WB Barton

January 2000



Prepared for the U.S. Department of Energy
under Contract DE-AC06-76RLO 1830

DISCLAIMER

This report was prepared as an account of work sponsored by an agency of the United States Government. Neither the United States Government nor any agency thereof, nor Battelle Memorial Institute, nor any of their employees, makes any warranty, express or implied, or assumes any legal liability or responsibility for the accuracy, completeness, or usefulness of any information, apparatus, product, or process disclosed, or represents that its use would not infringe privately owned rights. Reference herein to any specific commercial product, process, or service by trade name, trademark, manufacturer, or otherwise does not necessarily constitute or imply its endorsement, recommendation, or favoring by the United States Government or any agency thereof, or Battelle Memorial Institute. The views and opinions of authors expressed herein do not necessarily state or reflect those of the United States Government or any agency thereof.

PACIFIC NORTHWEST NATIONAL LABORATORY

operated by
BATTELLE

for the

UNITED STATES DEPARTMENT OF ENERGY

under Contract DE-AC06-76RLO 1830

Printed in the United States of America

Available to DOE and DOE contractors from the
Office of Scientific and Technical Information, P.O. Box 62, Oak Ridge, TN 37831;
prices available from (615) 576-8401.

Available to the public from the National Technical Information Service,
U.S. Department of Commerce, 5285 Port Royal Rd., Springfield, VA 22161



This document was printed on recycled paper.

(9/97)

DISCLAIMER

Portions of this document may be illegible in electronic image products. Images are produced from the best available original document.

Analysis of Several Hazardous Conditions for Large Transfer and Back-Dilution Sequences in Tank 241-SY-101

CW Stewart
LA Mahoney
WB Barton^(a)

January 2000

Prepared for
the U.S. Department of Energy
under Contract DE-AC06-76RLO 1830

Pacific Northwest National Laboratory
Richland, Washington

(a) CH₂M Hill Group, Inc.
Richland, WA 99352



Abstract

The first transfer of 89 kgal of waste and back-dilution of 61 kgal of water in Hanford Tank 241-SY-101 was accomplished December 18–20, 1999. Limits were placed on the transfer and back-dilution volumes because of concerns about potential gas release, crust sinking, and degradation of mixer pump performance. Additional transfers and back-dilutions are being planned that will bring the total to 500 kgal, which should dissolve a large fraction of the solids in the tank and dilute it well beyond the point where significant gas retention can occur. This report provides the technical bases for removing the limits on transfer and back-dilution volume by evaluating the potential consequences of several postulated hazardous conditions in view of the results of the first campaign and results of additional analyses of waste behavior.



Executive Summary

Four hazardous conditions created by crust sinking or dissolution were considered in this report: gas release by general bubble slurry flow through a thinned crust, gas retention due to crust encroachment on the mixer pump inlet, gas retention due to the inability of the mixer pump to mobilize a sunken crust, and ammonia evaporation from a free surface. The conclusions from analyses of both the flammability and toxicological hazards are discussed.

A bubble slurry release cannot create a flammable headspace under current or foreseeable conditions. If the postulated instantaneous bubble slurry release occurs during sinking, the headspace hydrogen concentration would be about 1.6%, or 45% of the LFL. If sinking does not occur, the release of the entire bubble slurry layer at this level would raise the headspace hydrogen concentration to 1.65%, 47% of the LFL. In either case, the thickness of the bubble slurry layer could double, and the gas release would still not exceed the LFL. Potential flammability due to a bubble slurry flow is dismissed as a hazard.

The corresponding ammonia release during either flow event, estimated by scaling up a recently observed flow, is 10 scm (356 scf), which would result in an ammonia concentration of 5300 ppm. Because small bubble slurry flows are apparently occurring regularly and since the existing and expected nonuniformity of crust thickness will prevent a sudden, complete release, this is very much a bounding value for bubble slurry flow.

If the crust begins sinking, it can stop descending short of the tank bottom only if it encounters fluid of a density sufficiently high to float the compressed material. A high-density layer that could support a sunken crust can potentially exist only just below the injection elevation. For low back-dilution, the injection point is the base of the transfer pump, at 96 inches. At this elevation, the crust would need to be 140 inches thick just to reach the main inlet. Because the crust is predicted to be only 64 inches thick when it sinks, we conclude that crust encroachment into the mixer pump by sinking cannot occur with low back-dilution.

If the crust sinks during top dilution, its thickness will be half that by low dilution, but the interface between the high- and low-density fluid will be only slightly above the main inlet after the second transfer. Therefore, the crust could theoretically stop descending at this level. This would not necessarily affect the mixer pump at all. However, if necessary, low back-dilution would raise the crust base to whatever level might be required to clear the inlet.

The hypothetical possibility that a segment of crust could "hang up" on the pump column around the inlet after waste level is lowered by the transfer is also discounted based on the behavior of the crust during the first campaign.

If the crust sinks by low back-dilution, the lower, weaker part will have dissolved, leaving the stronger layers. The mixer pump jet can mobilize this material to a radius of just over 4 meters, leaving over 87% of the sunken crust unmobilized and potentially able to retain gas. If a buoyant displacement gas release event (BD GRE) occurred after the third campaign, about 340 scm of gas would be released, which would bring the headspace hydrogen concentration to over 12%, over three times the LFL. If one-fourth of the sunken crust could become buoyant at one time and in view of the nonuniformity of the current crust, the hydrogen concentration would be just over 3%,

or 88% of the LFL, after the third campaign. It is more likely that the sunken crust would largely dissolve or be eroded away by repeated pump runs. The crust is actually not expected to sink at all but to break up into small segments. For all these reasons, we believe that the possibility of a sunken crust experiencing a large BD GRE is extremely remote.

When dissolved from the top down, the weaker portion, with a yield stress of 600 Pa, will remain. If this material were to sink, the mixer pump could have an effect on it out to a radius of over 9 meters, leaving only 32% not mobilized. The result of a BD GRE would raise the hydrogen concentration to just under 3%, 78% of the LFL. If we allow only one-fourth of the sunken crust to participate, as in the previous case, the resulting hydrogen concentration is only 0.7%, or 20% of the LFL. Based on this evaluation and being mindful of the long list of conservative assumptions required to create the scenario, BD GREs engendered by a sunken crust are dismissed as a hazard. Top back-dilution is recommended, however, because it has the least potential for gas retention.

When the crust dissolves, an exposed liquid pool might form that would allow ammonia to evaporate into the headspace at a rapid rate. When best estimates are used for the surface area exposed (50%) and the convective liquid velocity (which controls the mass transfer coefficient), the peak ammonia concentration is reduced to 4000 ppm. If the SY-101 headspace ammonia concentration begins to rise too high, a simple mitigating action is additional top-dilution water. Not only has the top dilution shown to be an effective scrubber of ammonia already in the headspace, the lighter water will float on top of the heavier brine to form an effective, if temporary, barrier to further evaporation.

A large transfer and back-dilution that effectively eliminates the current crust layer can be performed safely. While it is possible to create conditions that would exceed the LFL or produce high concentrations of ammonia in very specific hypothetical situations, we believe the list of improbably conservative assumptions required to make them happen is sufficiently long to make them incredible.

Contents

Abstract	iii
Executive Summary	v
1.0 Introduction	1.1
1.1 Conditions Following the First Transfer and Back-Dilution.....	1.1
1.2 Predictions of Crust Sinking.....	1.3
1.3 Hazardous Conditions Considered.....	1.3
2.0 Gas Release from Crust Thinning or Crust Breakup	2.1
2.1 Flammability Hazard of Bubble Slurry Flow	2.1
2.2 Observations of Gas Release During Slurry Flow Events	2.2
2.3 Ammonia Releases from Bubble Slurry Flow.....	2.6
3.0 Crust Encroachment into Mixer Pump Inlet.....	3.1
4.0 Inability to Mobilize Sunken Crust.....	4.1
4.1 Low Back-Dilution	4.1
4.2 Top Back-Dilution	4.4
5.0 Ammonia Release from an Exposed Liquid Pool.....	5.1
5.1 Ammonia Evaporation Model	5.1
5.2 Predicted Ammonia Concentrations	5.4
6.0 Summary and Conclusions.....	6.1
6.1 Flammability Hazard of Bubble Slurry Flow	6.1
6.2 Ammonia Releases from Bubble Slurry Flow.....	6.1
6.3 Crust Encroachment on the Mixer Pump Inlet	6.1
6.4 Inability to Mobilize Sunken Crust.....	6.2
6.5 Ammonia Evaporation from an Open Pool.....	6.3
6.6 Overall Conclusion	6.3
7.0 References	7.1

Figures

1.1	Crust at Riser 17B before and after the First Campaign	1.2
1.2	Crust at Riser 17C before and after the First Campaign	1.2
2.1a	VDTT 1B before Flow Event	2.3
2.1b	VDTT 1B after Flow Event	2.3
2.2a	VDTT 14A before Flow Event	2.4
2.2b	VDTT 14A after Flow Event	2.4
2.3	Gas Releases on January 7, 2000	2.5
2.4	Gas Releases on January 13, 2000	2.5
5.1	Headspace Ammonia Concentration versus Assumed Liquid Velocity	5.5
5.2	Headspace Ammonia Concentration versus Assumed Vapor Pressure	5.5
5.3	Headspace Ammonia Concentration versus Assumed Area	5.6

Tables

5.1	Waste Conditions for the Two Pool Evaporation Scenarios	5.2
5.2	Mass Transfer Parameters for the Two Scenarios.	5.3
5.3	Headspace Ammonia for Default Mass Transfer	5.4

1.0 Introduction

The first transfer and back-dilution in SY-101 was accomplished December 18–20, 1999. After an 89-kgal transfer, 26 kgal of water was added on top of the crust, followed by an addition of 35 kgal at the transfer pump inlet. Top dilution was limited to 25 kgal because of concerns about a potential gas release from the bubble slurry if the crust were thinned. Similarly, low back-dilution was limited to 75 kgal to prevent the crust from sinking. Concerns that the mixer pump would not be able to mobilize the sunken crust or that the crust would degrade mixer pump performance by encroaching on the main inlet led to placing this limit.

The second transfer is planned to be at least 210 kgal of waste,^(a) bringing the total to 300 kgal, with a roughly equal back-dilution with water. The crust should dissolve almost entirely during this back-dilution. After about 50 kgal have been added, it is expected to break up into islands and “wastebergs,” and some portion of it might sink. The cumulative 300-kgal dilution at the end of the second campaign will dissolve almost all of the readily soluble solids in the tank. A third transfer of 200 kgal with an equal back-dilution is being planned that will bring the total to 500 kgal. This will further dilute the remaining waste. This should be well beyond the point at which significant gas retention can occur.

This report provides the technical bases for removing the limits on transfer and back-dilution volume by evaluating the potential consequences of several postulated hazardous conditions in view of the results of the first campaign and results of additional analyses of waste behavior. Conditions after the first transfer and back-dilution are described in Section 1.1; crust sinking predictions are made in Section 1.2; and the hazardous conditions to be evaluated are discussed in Section 1.3.

1.1 Conditions Following the First Transfer and Back-Dilution

After the first transfer and back-dilution campaign, neutron probe data from Risers 17B and 17C indicate that the average crust thickness is 95–102 inches with the base at 305–315 inches and the surface level about 408 inches as shown in Figures 1.1 and 1.2, respectively. At the same time, the waste level was 404 inches at riser 1C and 417 inches at riser 1A. The crust buoyancy and dissolution model described in Rassat et al. (2000) predicts a crust thickness of 95 inches with the base at 314 inches and the surface at 408 inches.^(b)

(a) The second and third transfer volumes are intended to represent the volume of original, undiluted SY-101 mixed slurry. Therefore, actual transfer volumes will be somewhat larger than stated to correct for dilution.

(b) The original buoyancy model assumed that gas would be released from the mixed slurry in proportion to the fraction of solids that dissolved. This amount of gas release was not observed during the low back-dilution, and the predictions now assume that gas is not released from the mixed slurry. However, the difference in prediction is negligible.

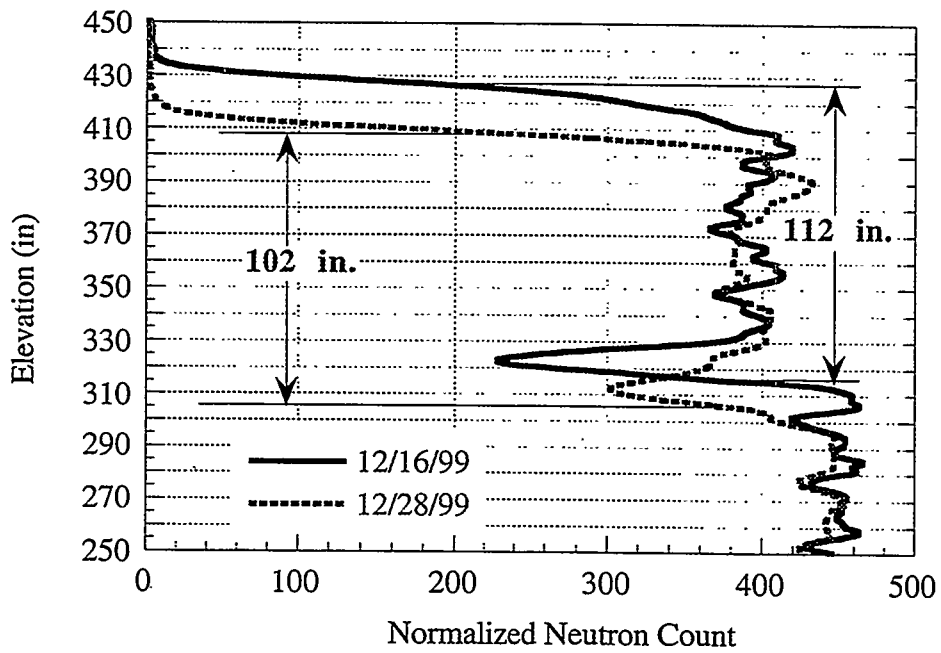


Figure 1.1. Crust at Riser 17B before and after the First Campaign

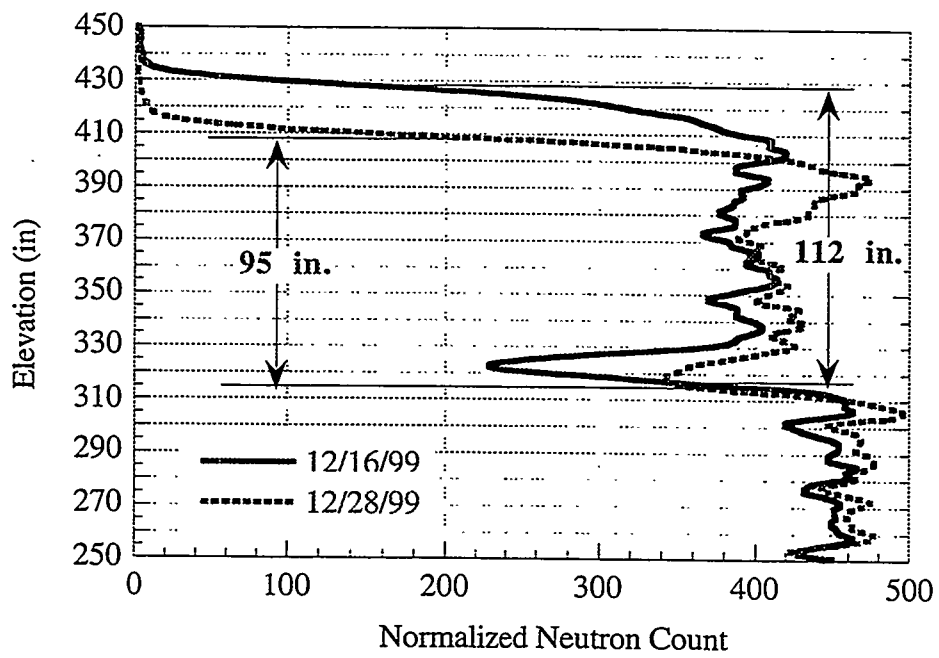


Figure 1.2. Crust at Riser 17C before and after the First Campaign

Only the top part of the crust experienced significant dissolution and the 10-inch bubble slurry layer at the crust base remains essentially intact. After several pump runs mixed the undiluted layer below 96 inches with the diluted upper portion, the mixed slurry remains saturated with a specific gravity of about 1.52. The mixer pump parameters indicate a slight improvement in performance since the back-dilution.

1.2 Predictions of Crust Sinking

The hazardous conditions under evaluation are all postulated results of the crust thinning or sinking. Under several conservative assumptions, the buoyancy model predicts that the crust will sink during back-dilution in the second campaign. Following the 210-kgal transfer, the crust is predicted to sink after 49 kgal of top back dilution^(a) or 28 kgal of low back-dilution through the transfer pump inlet. The crust thickness at sinking is predicted to be 30 inches if dissolution occurs from the top down by top dilution and 64 inches if it happens from the bottom up by low dilution. The thickness includes only the original crust. The insoluble solids that were assumed to remain on top after dissolution are assumed to disperse in the mixed slurry during sinking.

These conditions will be used as the best estimate for crust sinking conditions in subsequent analyses. The overall uncertainty of the low back-dilution volume required to sink the crust is estimated by a Monte Carlo analysis as a standard deviation of 12 kgal, or 20% of the total, by Rassat et al. (2000). The uncertainty analysis did not include top dilution and considers only the propagation of input uncertainty. For low dilution, the corresponding uncertainty in crust thickness at sinking is significantly less than that of the volume. The standard deviation is about 10% of the final crust thickness.^(b) At the same time, the actual crust dissolution and changes in buoyancy resulting from the first campaign matched the model's predictions quite well. For these reasons and because the analysis is already quite conservative, we chose not to adjust the predictions of crust thickness at sinking in an attempt to bound the uncertainty.

The entire crust is assumed to sink as an intact disk without breaking up into segments, even though the observed nonuniformity of the existing crust and of the dilution process make this quite unrealistic. We assume that the bubble slurry layer, if any, is destroyed during the sinking process and only the paste layer remains. The crust is assumed to sink onto the top of the loosely settled layer. Validation probe temperature profiles at a 27–29 ft radius from the mixer pump show that this layer is 40–50 inches thick (Stewart et al. 1998; Rassat et al. 2000). The greater thickness is assumed to apply over the entire tank even though it is almost certainly much thinner closer to the mixer pump. The combination of these assumptions makes the analyses extremely conservative.

1.3 Hazardous Conditions Considered

Four hazardous conditions are considered in this report: gas release by general bubble slurry flow through a thinned crust, gas retention due to crust encroachment on the mixer pump inlet,

(a) The crust is predicted to sink by top dilution mainly due to the assumed accumulation of insoluble solids that stay on top as weight while the soluble solids dissolve and flow away.

(b) Calculated from simulation outputs provided by Stacey Hartley, PNNL.

gas retention due to the inability of the mixer pump to mobilize a sunken crust, and ammonia evaporation from a free surface. Both flammability and toxicological hazards are considered. The hazard scenarios are explained in more detail below.

The bubble slurry is thought to be a relatively weak, potentially fluid, high-void layer lying under the stronger part of the crust. Water added on top of the crust is expected to dissolve the crust from the top down. If the crust is thinned sufficiently, it is postulated that the bubble slurry could erupt through it, releasing its retained gas and thereby making the headspace flammable. The corelease of ammonia can also create a toxicological hazard to operators. Both aspects were analyzed previously based on the scenario of bubble slurry flow up through a large, clean, hole in the crust.^(a,b) However, the consequences of a wide-area bubble slurry flow due to crust thinning was not considered. In Section 2, a bounding 100% release of the bubble slurry layer is shown to remain below the lower flammability limit. A recently observed bubble slurry flow is scaled up to predict the associated ammonia concentrations.

If the crust were to sink such that it surrounded the mixer pump inlet, it is postulated that the mixer pump could be disabled by plugging or its performance degraded by ingestion of gas and solids. If this degradation were severe, it might prevent adequate mobilization of settled solids, permitting gas retention and eventual return to buoyant displacement gas release events (BD GREs). Section 3 analyzes the hazard by considering the dimensions of the crust at sinking and the potential density stratification in the mixed slurry. It is shown to be impossible for a sinking crust to encroach on the mixer pump except for one case of top dilution where the crust is much thinned before sinking.

If the crust sinks and retains its relatively high strength after sinking, the mixer pump jet may not be able to mobilize it. If this should continue for many months, the unmobilized sections of the sunken crust could retain enough gas to become buoyant and experience a BD GRE. Depending on how thick the crust is when it sinks and how many conservative assumptions are applied, the gas release volumes could cause the headspace to exceed the lower flammability limit (LFL). Section 4 considers the estimated strength of different layers of the crust and the dynamics of the mixer pump jet to calculate the radius to which the jet can mobilize the sunken material. Sinking by both low dilution and top dilution are considered. The various bounding assumptions that make the gas retention scenario possible are evaluated qualitatively.

Up to now, the crust has provided a barrier against ammonia evaporation. When the crust dissolves or sinks, an exposed liquid pool might hypothetically form that would allow ammonia to evaporate into the headspace at a rapid rate. This release could continue indefinitely unless it was retarded by a new crust or foam forming over the exposed liquid. Section 5 estimates the evaporative release and resulting headspace concentration of ammonia assuming the entire tank area is an open pool. Conditions that are likely to reduce the ammonia concentration significantly are described.

(a) Meyer PA, CW Stewart, SD Rassat, RT Allemann, G Terrones and DP Mendoza. May 1999. . PNNL Letter Report TWS99.27, Rev. 1, *Potential Gas Release by Bubble Slurry Flow Through a Hole in the Crust Layer in SY-101*, Pacific Northwest National Laboratory, Richland, Washington.

(b) Mahoney LA, PA Meyer and CW Stewart. May 1999. PNNL Letter Report TWS99.35, *Ammonia Release from Bubble Slurry Flow Through a Hole in the Crust Layer in SY-101*, Pacific Northwest National Laboratory, Richland, Washington.

Conclusions are summarized in Section 6, and references are listed in Section 7. The overall conclusion is that a large transfer and back-dilution that is expected to effectively eliminate the current crust layer can be performed safely. While it is possible to create conditions that would exceed the LFL or produce high concentrations of ammonia in very specific hypothetical situations, we believe the list of improbably conservative assumptions required to make them happen is sufficiently long to make them incredible.

2.0 Gas Release from Crust Thinning or Crust Breakup

The bubble slurry is thought to be a relatively weak, potentially fluid, high-void layer lying under the stronger part of the crust. Water added on top of the crust is expected to dissolve the crust from the top down. If the crust is thinned sufficiently, it is postulated that the bubble slurry could erupt through it, releasing its retained gas and thereby making the headspace flammable. The corelease of ammonia can also create a toxicological hazard to operators. This section addresses both flammability and toxicology hazards and describes recent events that are believed to be bubble slurry flows.

2.1 Flammability Hazard of Bubble Slurry Flow

A bubble slurry release cannot create a flammable headspace under current or foreseeable conditions. A bubble slurry layer 10 inches thick (as indicated by the neutron probe data) with a void fraction of 0.6 under a pressure of 1.3 atm contains 80 scm of gas, assuming it spans the entire tank. If all of the gas were released instantaneously at a waste level of 429 inches, the headspace hydrogen would just reach the LFL,^(a) assuming well-mixed conditions.^(b) However, the waste level is currently about 410 inches and will be much less by the time a bubble slurry release could occur.

A bubble slurry release could occur by sinking or when the paste layer above becomes too thin. After the second transfer of over 200 kgal of waste, the level will drop by more than 70 inches. If the crust is assumed to sink as predicted after 49 kgal of top back-dilution, the paste layer is predicted to be 20 inches thick, and the surface level will be about 330 inches. The bubble slurry layer remains intact at this point (Rassat et al. 2000). If the postulated instantaneous bubble slurry release occurs during sinking, the headspace hydrogen concentration would be about 1.6%, or 45% of the LFL.

If sinking does not occur, the paste layer is predicted to be fully dissolved after another 15 kgal of top back-dilution, which would raise the surface level to about 335 inches. This would be the highest waste level and therefore the smallest headspace volume into which a complete bubble slurry release could occur. Here the release of the entire bubble slurry layer would raise the headspace hydrogen concentration to 1.65%, 47% of the LFL. In either case, the thickness of the bubble slurry layer could double, and the gas release would still not exceed the LFL.

The actual release would be much less than the total of 80 scm. Bubble slurry would not be released uniformly from the entire tank cross-section. The effect of dissolution in Campaign #1 was nonuniform, as evidenced by difference in neutron profiles and temperature histories at the MITs in risers 17B and 17C and the differing waste levels registered by the four instruments, as described in Section 1. The additional dissolution required before bubble slurry release can occur is expected to increase the nonuniformity. Bubble slurry flow would not be instantaneous due to

(a) For the measured SY-101 gas composition (Mahoney et al. 1999) of 38% hydrogen (LFL = 4%) and 12% ammonia (LFL = 15%), LeChatellier's rule gives an LFL of 3.5% hydrogen.

(b) Gas release from the postulated slurry flow would be from a wide area, so headspace should be well mixed. Neither flammable plume nor stratified layer would exist in the Epstein model (Slezak et al. 1998).

the low hydrostatic pressure difference driving the slurry layer to waste surface. The actual release time might be hours. Gas release from the bubble slurry flow would not be complete. Typically a 50% release fraction is assumed for energetic releases and the low-pressure difference for the thinned crust would not make a bubble slurry flow very energetic. However, even a 50% release fraction would lower the maximum result above to less than 25% of the LFL. Because a bubble slurry release cannot create a flammable headspace, even under unrealistic bounding conditions, it can be dismissed as a hazard during future back-dilutions.

2.2 Observations of Gas Release During Slurry Flow Events

The SY-101 in-tank camera clearly shows that there have been flows of waste across the surface of SY-101 since the first transfer/dilution on December 18–21, 1999. The largest flow observed thus far occurred between 15:59 on Friday, January 7, and 13:45 on Saturday, January 8, 2000. These times are based on captured screen images from the in-tank camera. A full-tank surface scan was performed on Monday, January 10. It recorded a flow of foamy waste on the surface, believed to be the bubble slurry, that covered a large area of the waste. Although no measurements of the actual size of the flow are possible, it is estimated to cover 1–2% of the tank area. Examples of flows around each of the two velocity-density-temperature trees (VDTTs) in risers 1B and 14A are shown in Figures 2.1a and 2.1b and Figures 2.2a and 2.2b, respectively.

Two gas-release spikes occurred during that time period, as shown in Figure 2.3. The first was the normal expected spike following a mixer pump run (note the slight increase shortly after 14:00 is attributed to the disturbance caused by pump column rotation). The pump was run at 14:40 on January 7 with the released gases peaking at 15:34. The hydrogen peaked at concentration of 124 ppm. As this peak was decaying, another spike occurred at 18:22 with a peak hydrogen concentration of 384 ppm. The second peak is believed to be associated with the waste flow discussed above. This waste flow did not result in extremely high concentrations of any of the gases monitored. Because the first video images in which no flow was observed were captured after the peak gas concentrations following the pump run, it can be safely assumed that the flows observed in the 13:45 January 8 video result from the same event that caused the 18:22 January 7 gas spikes.

Review of the January 10 full in-tank video scan showed evidence of at least five separated waste flows of varying sizes (none larger than about 2% of the tank surface) have occurred since the transfer. The gas monitoring has shown at least four releases not associated with pump runs since January 1 and ten or more between December 21 and January 1. Figure 2.4 shows an example of a smaller release following the pump run on January 13. The spontaneous gas releases are comparable in size to those seen in mixer pump runs. It is believed that the spontaneous gas releases are generally associated with the waste flows seen in the tank scan. The number of events does not correlate with the number of flows because multiple releases probably came from the same location, and the camera cannot see details on the opposite side of the tank.



Figure 2.1a. VDTT 1B before Flow Event



Figure 2.1b. VDTT 1B after Flow Event

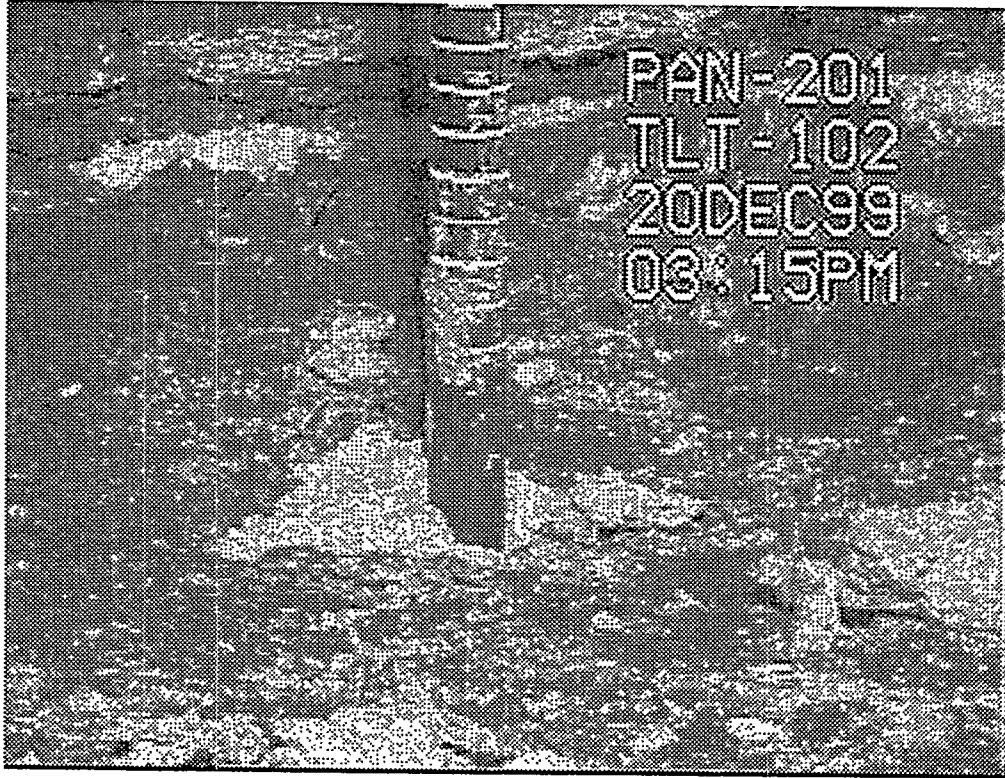


Figure 2.2a. VDTT 14A before Flow Event

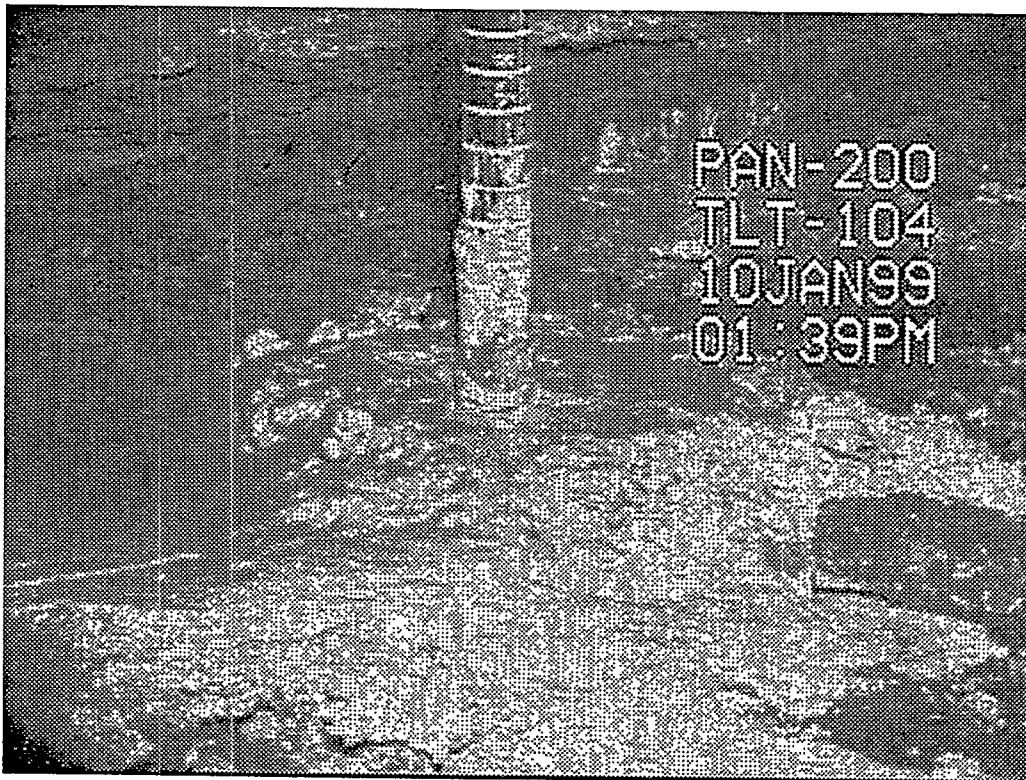


Figure 2.2b. VDTT 14A after Flow Event

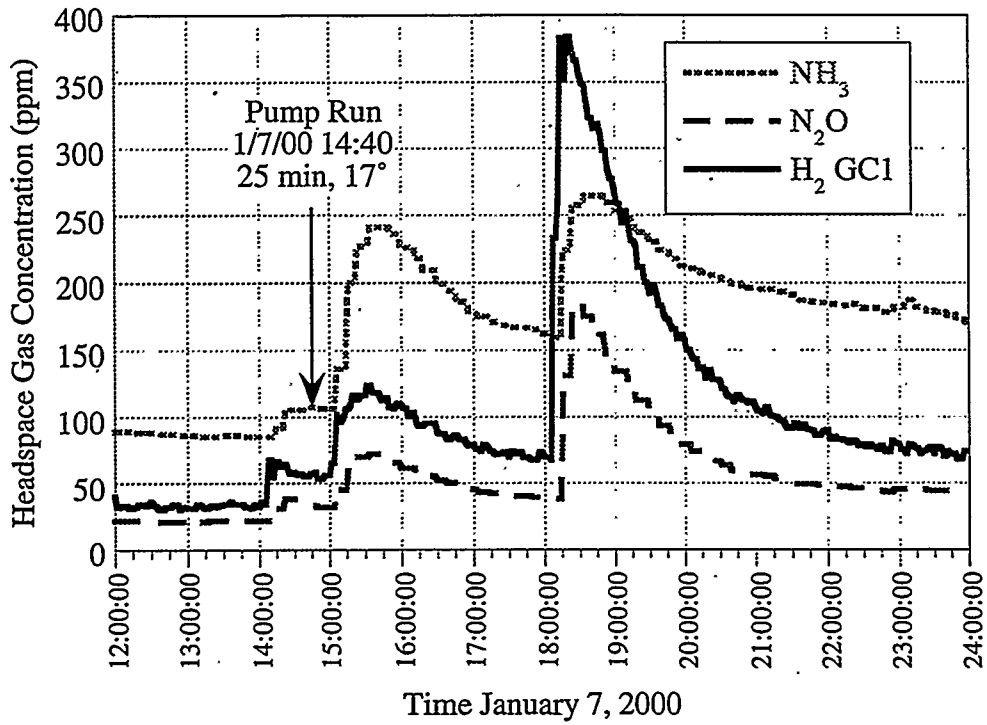


Figure 2.3. Gas Releases on January 7, 2000

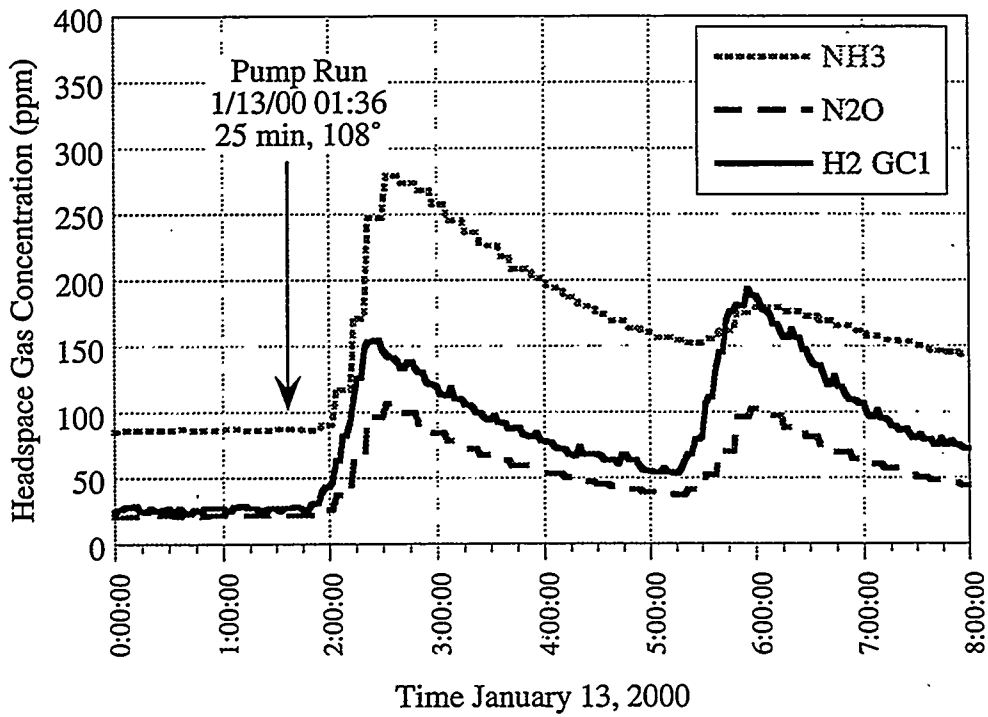


Figure 2.4. Gas Releases on January 13, 2000

2.3 Ammonia Releases from Bubble Slurry Flow

Ammonia releases are a potential toxicological hazard to operators in the tank farm. Elevated ammonia concentrations are expected during and after a bubble slurry flow due to evaporation from the wet, newly exposed surface. An earlier analysis of bubble slurry flow gas release was based on the conservative assumption of a large, clean hole in the crust allowing a semi-fluid bubble slurry to flow rapidly from the crust base to the crust surface.^(a) Ammonia releases from this idealized bubble slurry flow model were estimated^(b) based on the ammonia concentrations from the retained gas sampler (RGS) data obtained in November 1998 through January 1999 (Mahoney et al. 1999). For a 50-cm (20-inch) bubble slurry layer and a 2.5-m (100-inch) thick crust, the peak ammonia concentration was predicted to be 6400 ppm.

Rather than re-running this model for the current 25-cm (10-inch) bubble slurry, we used the data given in Section 2.2 to scale up the ammonia release from an actual bubble slurry flow event to match a larger event including the entire bubble slurry volume. The scale-up factor is simply the ratio of the actual January 7 gas release volume to the total bubble slurry gas volume. The latter was established in Section 2.1 as 80 scm (2,825 scf). The total gas release volume from the flow event can be calculated as

$$V_{\text{REL}} = V_{\text{HS}} \frac{\Delta[\text{H}_2]_{\text{HS}}}{\chi_{\text{H}_2}} \quad (2.1)$$

where V_{REL} is the total release volume, V_{HS} is the tank headspace volume, $\Delta[\text{H}_2]_{\text{HS}}$ is the change in headspace hydrogen concentration as it rises to its peak, and χ_{H_2} is the fraction of hydrogen in the release gas. The ammonia release is computed similarly by

$$V_{\text{NH}_3} = V_{\text{HS}} \Delta[\text{NH}_3]_{\text{HS}} \quad (2.2)$$

Equations (2.1) and (2.2) provide estimates that are about 90% of the total gas release that can be calculated by a detailed integration of the headspace concentration history.^(c) They are lower bounds of the gas release because they represent the minimum, instantaneously released gas volume needed to produce the measured change in headspace concentration. The additional gas that is exhausted by ventilation during the rise to peak concentration or that released after the peak is ignored. However, the lower bound is conservative in this case because it will give the highest scale-up factor.

During the January 7 flow event the average waste level was 410 inches, which makes the tank headspace volume 1063 m³ (37,500 ft³). A minimum of 0.89 scm (31 scf) of gas containing 38%

(a) Meyer PA, CW Stewart, SD Rassat, RT Allemann, G Terrones, and DP Mendoza. May 1999. Letter Report TWS99.27 Rev. 1, *Potential Gas Release by Bubble Slurry Flow Through a Hole in the Crust Layer in SY-101*, Pacific Northwest National Laboratory, Richland, Washington.

(b) Mahoney LA, PA Meyer, and CW Stewart. May 1999. Letter Report TWS99.35, *Ammonia Release from Bubble Slurry Flow Through a Hole in the Crust Layer in SY-101*, Pacific Northwest National Laboratory, Richland, Washington.

(c) Personal communication with WB Barton, CHGI.

hydrogen was released into this headspace to raise the hydrogen concentration from 67 to 384 ppm (see Figure 2.2). This is 1/90 of the 80 scm contained in the 10-inch bubble slurry layer.

The corresponding ammonia release during the flow event was 0.11 scm (3.9 scf). Multiplying this release volume by the scale-up factor of 90 yields an estimate of 10 scm (356 scf) for the ammonia release from the entire bubble slurry layer. The bubble slurry is postulated to be released due to crust thinning by top dilution or crust sinking. The minimum headspace and therefore the maximum ammonia concentration would result if the slurry flow happened just before crust sinking. Assuming a 300-kgal total transfer (89 kgal in Campaign #1 and 211 kgal in Campaign #2), the waste level at sinking is predicted to be 330 inches, for a headspace volume of 1900 m³ (67,000 ft³). If the 10 scm of ammonia is instantaneously released into this volume, the resulting concentration is 5300 ppm. This is consistent with the 6400 ppm predicted in the earlier calculation.

Because small bubble slurry flows are apparently occurring regularly, and the existing and expected nonuniformity of crust thickness will prevent a sudden, complete release, the predicted 5,300-ppm ammonia concentration is very much a bounding value for bubble slurry flow. The ammonia concentration predicted due to evaporation of a liquid surface in the absence of the crust is much higher. This mechanism is discussed in Section 5.

3.0 Crust Encroachment into Mixer Pump Inlet

It is postulated that the mixer pump could be disabled by plugging or its performance degraded by ingestion of gas and solids if the crust were to sink and surround the mixer pump inlet. It is further postulated that this degradation might prevent adequate mobilization of settled solids and thus permit gas retention and eventual return to BD GREs.

If the crust begins sinking, it will accelerate as the increasing hydrostatic pressure compresses the retained gas. The crust can stop descending short of the tank bottom only if it encounters fluid of a high-enough density to float the compressed material. Modeling predictions and temperature profile data following low back-dilution in the first campaign indicate that mixing above the dilution injection point is good while the fluid below the injection point is essentially unmixed. Therefore, a high-density layer that could support a sunken crust can potentially exist only just below the injection elevation.

It is also hypothetically possible that a segment of crust could “hang up” on the pump column surrounding the inlet after waste level is lowered by the transfer. However, this possibility is discounted for the following reasons:

- The base of the crust will remain be above the mixer pump inlet, even after the maximum possible transfer, given the current waste level, the capacity of SY-102 and in-line dilution requirements.
- The crust fell and rose smoothly around the mixer pump column during the first transfer and back-dilution with no hint of a hang-up. Both top and bottom dilution were observed to raise the crust positively and smoothly.
- If the crust could descend around the pump column to the level of the inlet without binding, there would no reason to expect it to bind there.

A transient “hang-up” of a segment of the crust around the mixer pump inlet during the sinking process is considered even less plausible for the same reasons.

As will be shown, the crust is predicted to be thickest on sinking if dissolution is from the bottom up by low back-dilution. It is predicted to sink when the slurry specific gravity is 1.45 at a 64-inch thickness. At that time the undiluted slurry below the transfer pump inlet at 96 inches will have a specific gravity of 1.52, assuming the mixer pump has not been run since the start of the second campaign. Using the ideal gas law and the definition of the void fraction, the change in void with pressure can be expressed as

$$\alpha_1 = \left[1 + \frac{(1 - \alpha_0) P_1}{\alpha_0 P_0} \right]^{-1} \quad (3.1)$$

where α_0 and α_1 are the void fractions corresponding to pressures P_0 and P_1 , respectively. The crust density is given by

$$\rho = (1 - \alpha)\rho_{DG} \quad (3.2)$$

where ρ_{DG} is the degassed crust density. The pressure is related to the sinking depth, ΔH , by

$$P = P_a + \rho_{CL}g\Delta H \quad (3.3)$$

where P_a is the barometric pressure, ρ_{CL} is the convective layer density, and g is the acceleration of gravity. Combining Equations (3.1), (3.2), and (3.3), the increase in crust density with pressure can be determined by

$$\rho_1 = \rho_{DG} \left\{ 1 - \left[1 + \frac{\rho_0}{(\rho_{DG} - \rho_0)} \frac{(P_a + \rho_{CL}g\Delta H_1)}{(P_a + \rho_{CL}g\Delta H_0)} \right]^{-1} \right\} \quad (3.4)$$

Where ρ_0 and ρ_1 are the initial and final crust densities corresponding to initial and final crust midpoint depths, ΔH_0 and ΔH_1 , respectively. Equation (3.4) predicts that the average specific gravity will increase from 1.45 as it begins to sink to 1.56 when its base reaches 96 inches. Because the slurry specific gravity below the transfer pump inlet is only 1.52, it cannot support the sinking crust.

Therefore, we can assume that the descending crust stops only upon contacting the loosely settled layer, 50 inches off the tank bottom (ignoring any compaction). This places the top of the 64-inch sunken crust at an elevation of 114 inches, 122 inches below the mixer pump inlet at the 236-inch elevation.^(a) The crust thickness would have to be greater than 186 inches to reach from the top of the loosely settled layer to the inlet, much less surround it. Even if it did stop with its base at 96 inches, the crust would have to be 140 inches thick just to reach the main inlet.^(b) Since the crust thickness before any thinning by back-dilution in the first campaign was only 120 inches, and is now estimated to be up to 25 inches thinner (see Section 1), we conclude that crust encroachment into the mixer pump cannot occur by any sinking scenario with low back dilution.

If the crust sinks during top dilution, its thickness will be half that by low dilution, but the interface between the high- and low-density fluid will be very close to the pump inlet. The crust base will be only slightly above the main inlet after the second transfer. As water is added on top of the crust, it flows under the crust when it becomes dense enough for the crust to float. This means that the specific gravity of this fluid will be slightly less than that of the initial slurry density, which is predicted to be about 1.52 after the second transfer. The crust is expected to sink when its specific gravity reaches 1.45 with its upper surface at about 330 inches and its base at 300 inches.

In this situation, with less than 70 inches to sink, Equation (3.4) predicts that the crust specific gravity will have increased only to about 1.48. Thus it would theoretically float at the level of the mixer pump inlet. However, even with such a short drop, the energy ratio (energy released to that required to yield the waste) for the bubble slurry is about 6 according to the derivation of Rassat et al. (2000) if its yield stress is 100 Pa. If the bubble slurry releases its gas as expected, the specific

(a) RE Raymond (LMHC). August 18, 1999. Interoffice Memo 79000-99-053, 241-SY-101 Mixer Pump Main Inlet Level.

(b) Actually, the crust would need to sink partially into the high-density layer to provide the buoyant force to arrest sinking.

gravity of the crust becomes 1.58, allowing it to sink easily past the mixer pump inlet through the 1.52-specific gravity mixed slurry. If the bubble slurry was not released and the crust did sink just to the mixer pump inlet, low back-dilution would raise it to whatever level is required to clear the inlet. Sufficient low back-dilution would also reduce the slurry density to the point that a partially sunken crust would complete its descent to the bottom.

We conclude that, while crust sinking from top back-dilution hypothetically has the potential to encroach on the mixer pump inlet, any mixer pump performance degradation can be reversed by a small volume of low back-dilution and therefore does not constitute a hazard.

4.0 Inability to Mobilize Sunken Crust

If the average density of a portion of the crust becomes greater than that of the mixed slurry, it will sink until it encounters either fluid with a density sufficient to support it or the tank bottom. It is postulated that the sunken crust may remain sufficiently strong that the mixer pump jet cannot mobilize it to prevent gas retention. If this should occur, it is further postulated that unmobilized sections of the sunken crust could become buoyant and exhibit BD GREs.

The consequences of crust sinking will be evaluated by estimating the maximum possible gas release from an unmobilized portion of a sunken crust under a series of conservative assumptions. Section 4.1 considers the case of sinking resulting from low back dilution and Section 4.2 treats sinking by top back-dilution. Both sections evaluate conditions after both the second campaigns.

4.1 Low Back-Dilution

The result of crust sinking due to low back-dilution onto the 50-inch loosely settled layer is a nonconvective layer 114 inches thick immediately after sinking. The mixer pump will be able to mobilize at least the central part of this layer. The mixer pump jet penetration radius depends on the material yield strength, jet velocity and diameter, and the density of the fluid in the jet. After back-dilution reaches a total of 300 kgal in the second campaign, the slurry density will have been diluted to a specific gravity of 1.41. Since low dilution will have dissolved the crust from the bottom up, eliminating the weakest material first, we assume the sunken crust has the maximum yield strength computed for the paste layer of 3000 Pa (Rassat et al. 2000). Under these conditions, it can be mobilized to a radius of just over 4 meters with the mixer pump running at 1000 rpm. This leaves over 87% unmobilized, equivalent to a cylindrical gob 21.3 m in diameter.

The unmobilized portion of the crust is assumed to be a uniform ring of rectangular cross-section. It is conservatively assumed that the loosely settled layer on which the sunken crust rests is protected from the jet and not mobilized beyond the radius computed for the stronger material. Gas retention to the point of buoyancy will require many months; therefore, if the current schedule holds, this condition could not occur until after the third campaign. The additional 200-kgal transfer and back-dilution will lower the slurry specific gravity to about 1.26. The unmobilized ring of sunken crust is very conservatively assumed not to dissolve by this highly subsaturated liquid nor eroded beyond the initial radius by additional mixer pump runs.

The ring of sunken crust contains a very large gas volume. Because the liquid is so dilute, the neutral buoyancy void fraction is over 0.25. The original crust paste layer had an average void fraction of about 0.2 and the loosely settled layer void is assumed to be the same as that of the mixed slurry, 0.03, for an average of 0.13. Expansion to the neutral buoyancy void fraction increases the thickness from the original 114 inches to 135 inches and the waste level increases to about 412 inches. At neutral buoyancy, the total retained gas volume is over 650 scm.

If for some reason the third transfer and back dilution campaign is not performed, the slurry will be less diluted, which would significantly reduce the potential retained gas volume. With the estimated 1.41 specific gravity after the second campaign, the neutral buoyancy void fraction is 0.17. This reduces the expanded thickness of the sunken crust to 120 inches and the waste level to

398 inches. A neutral buoyancy condition after the second campaign would retain 400 scm, just 62% of the retention possible after the third campaign.

The sunken crust is assumed to release gas as in a BD GRE. That is, it retains generated gas until it becomes buoyant with respect to the fluid above it, rises to the surface as a unit, and releases gas until it becomes negatively buoyant again (Meyer et al. 1997). The fraction of the total gas released in this way is given by

$$F_R = 1 - \frac{P_a}{P_G} \quad (4.1)$$

where P_a is the ambient barometric pressure and P_G is the average in-situ pressure of the gas. The buoyant potential energy is so high due to the high neutral buoyancy void fraction that, even with the high yield stress, the energy ratio is well above that necessary for an energetic release. Therefore, the gas release is assumed to be instantaneous and the tank headspace well mixed.

If a BD GRE occurs after the third campaign, the computed in situ gas pressure is 2.1 atm, and the release fraction is 0.52. About 340 scm of gas would be released, which would bring the headspace hydrogen concentration to over 12%. This is over three times the LFL of 3.5% hydrogen. If the third campaign is not performed, the GRE would have a release fraction of 0.54, and 220 scm of gas would be released. This would result in a headspace hydrogen concentration of 7%, exactly twice the LFL.

However, it is unlikely that the entire volume would act as a unit. Consider the nonuniformity of the current crust. The surface levels vary from 417 inches at riser 1A to 405 inches at riser 1C, with risers 17B and 17C showing 410 inches. The crust thickness is also nonuniform. Further dissolution during the second campaign will make the crust more nonuniform. Therefore, the entire crust cannot be assumed to dissolve uniformly and sink at the same time, even though it has been assumed so, nor to uniformly resist mobilization and become buoyant at the same time.

Though it is reasonable to expect that the entire ring would not go simultaneously, it is impossible to calculate exactly how much of it would. The gob size model of Meyer et al. (1997) does not fit this geometry, and the assumed strength of 3000 Pa violates an enabling assumption that the gas-bearing material behaves as a quasi-fluid. This also prevents a direct comparison to the 10–12-m gob diameters exhibited by SY-101 prior to mixing. It would seem reasonable to limit the buoyant gob to one-fourth of the unmobilized ring. One fourth of the total gas release after the third campaign results in a hydrogen concentration just over 3%, or 88% of the LFL. One-fourth of the gas release under post-second campaign conditions would produce 50% of the LFL.

This is a very slim margin. However, it is also the result of a series of unrealistic conservatisms. Consider the following list of conservative assumptions that are made in addition to that of complete uniformity:

- Maximum yield stress of 3000 Pa is applied, and strength is not reduced by heating, dissolution, unloading or gas generation.

- The loosely settled layer is assumed trapped by the crust, not compacted and not mobilized beyond the crust's theoretical radius even though it is normally swept away by the jet.
- Sunken crust is not dissolved after it sinks even though exposed for months to highly subsaturated fluid.
- Sunken crust is not eroded or dissolved beyond the theoretical radius by repeated pump runs even though the original waste was excavated in proportion to cumulative runs.

Removing the first assumption and allowing the crust strength to weaken to 600 Pa, or removing the second assumption and eliminating the loosely settled layer from the BD GRE would roughly double the margin to the LFL. Removing both would reduce the worst case to 65% of the LFL. Removing the last two assumptions would probably allow the entire sunken crust to be mobilized or dissolved.

The crust is actually not expected to sink at all. Several experiments and analyses by Rassat et al. (2000) show that dissolution should tend to break up the crust into small segments. Experiments with a nonradioactive chemical simulant matching SY-101 waste composition indicate that the crust dissolves nonuniformly to form smaller "wastebergs" or "dumplings" that continue to float as they dissolve. A slightly larger-scale experiment, in which a tray of sugar and molasses was dissolved by water dripped at a point, showed a highly nonuniform "fingering" pattern. Basic convective mass transfer theory also predicts that dissolution will tend to widen existing passages and cavities rather than thin the crust uniformly.

Even if the crust should sink, it cannot remain impervious to the mixer pump jet. Though portions of the floating crust are quite strong, the material will tend to weaken significantly should it sink. The strength of a particulate medium increases with lithostatic load that compacts the matrix of particles together. The compaction force is actually much greater when the crust is floating than when it is submerged. Besides the effect of reduction in lithostatic load, the material will also weaken in situ by expansion as gas accumulates. The material will also be at a higher temperature, which further dissolves solids and reduces the viscosity of the liquid. If the sunken crust's strength is reduced to 400 Pa, still stronger than the average strength of the original nonconvective waste, the mixer pump could reach all the way to the wall.

The mixer pump will perform better as dilution proceeds and the mixed slurry becomes less dense and less viscous. Addition of 35 kgal at the transfer pump inlet measurably reduced the mixer pump power and lowered the peak motor oil temperature at the end of the first several 25-minute runs following the first campaign. Further dilution will make it possible to run the mixer pump longer and/or at a higher speed, which will increase the radius of mobilization. Increasing the motor speed from 1000 rpm to 1200 rpm increases the jet penetration by about 20%.

For all these reasons, we believe that, despite the results of the very conservative analysis, crust sinking by low dilution will not actually create conditions that would degrade the mixer pump's ability to mitigate gas retention. The possibility of a sunken crust experiencing a large BD GRE is extremely remote.

4.2 Top Back-Dilution

When dissolved from the top down, the crust is much thinner when it is predicted to sink than if dissolved by bottom-up back-dilution. The crust thickness is only 30 inches, of which 10 inches is the bubble slurry layer that is assumed to disintegrate during sinking. With the 50-inch loosely settled layer, the resulting nonconvective layer is 70 inches thick immediately after sinking. The sunken crust is also much weaker because the stronger top portion has been dissolved. Rassat et al. (2000) estimate the lower part of the paste layer to have a yield stress from 400 to 600 Pa. We assume the higher value.

The mixer pump should be able to mobilize most of this layer easily by tunneling under the sunken crust through the loosely settled layer. However, we shall assume that penetration is limited by the maximum strength. After the second campaign, the slurry density has a specific gravity of 1.44. This is slightly higher than for low dilution because more of the crust has been dissolved. Under these conditions, the sunken crust can be mobilized to a radius of over 9 meters. This leaves only 32% unmobilized, equivalent to a cylindrical gob 13 m in diameter.

The third transfer and back-dilution lowers the slurry specific gravity to about 1.3. This is also slightly higher than that for low water addition because more of the crust has been dissolved. The higher slurry density reduces the neutral buoyancy void fraction from over 0.25 to 0.235.

The sunken crust contains a much smaller gas volume than it does for low addition. The initial average void of 20 inches of paste layer at a void fraction of 0.20 and the loosely settled layer at an assumed 0.03 void fraction is 0.08. Expansion to the neutral buoyancy void fraction of 0.235 increases the thickness from the original 70 inches to 84 inches, and the waste level grows to about 406 inches. The release fraction is 0.54. At neutral buoyancy, the total releasable gas is just under 80 scm. If this volume is released instantaneously into the headspace at the 409-inch level, the hydrogen concentration is just under 3%, 78% of the LFL. If we allow only one-fourth of the sunken crust to participate, as in the previous case, the resulting hydrogen concentration is only 0.7%, 20% of the LFL. For post-second campaign conditions, the maximum instantaneous release would reach less than 50% of the LFL.

Based on the above evaluation, and noting again the long list of conservative assumptions required to create the scenario (see Section 4.1), BD GREs engendered by a sunken crust are dismissed as a hazard. However, top back-dilution is recommended because it results in the least potential for gas retention.

5.0 Ammonia Release from an Exposed Liquid Pool

One result of dilution is expected to be the thinning or submergence of the crust, which up to now has provided a barrier against ammonia evaporation. When the crust dissolves, an exposed liquid pool might form that would allow ammonia to evaporate into the headspace at a rapid rate. This release could continue as long as ammonia remained, unless mass transfer was retarded by a new crust or foam forming over the exposed liquid. The object of this section is to estimate the evaporative release and resulting headspace concentration of ammonia.

We have modeled two scenarios for the ammonia release in which the entire liquid area is assumed to be exposed. The first scenario is that of a 300-kgal transfer and 113-kgal dilution (35 kgal low and 78 kgal on top), the point at which the crust is predicted to sink.^(a) This is the first opportunity for an exposed pool. At this time, the dissolved ammonia concentration is the highest, but the headspace is the largest. The ammonia concentrations are based on the average values measured in SY-101 slurry and crust samples by retained gas sampling (Mahoney et al. 1999).

The second scenario is that of 300-kgal transfer with an equal back-dilution. In this case, the dissolved ammonia is somewhat more dilute, but the headspace volume is smaller than in the first scenario. Table 5.1 lists the configurations and waste properties that were used in the two scenarios and in the initial pretransfer condition. The initial conditions (other than the ammonia and salt concentrations) were taken from Rassat et al. (2000).

5.1 Ammonia Evaporation Model

Solids dissolution is modeled by assuming that 1.267 g of soluble solids are dissolved per gram of water (Rassat et al. 2000). Top-dilution water is assumed to dissolve crust solids then become part of the slurry. There, any excess water dissolves solids in the slurry. The top-dilution water is assumed to carry the ammonia present in the brine within the crust into the slurry with it, in proportion to the ratio of the dilution water to the sum of dilution water plus brine originally in the crust. Bottom-dilution water is assumed to dissolve slurry solids and (if in excess) then to dissolve crust solids. Once all the soluble solids in the crust are dissolved, the remaining gas, ammonia, and insoluble solids from the crust are considered part of the slurry. The slurry is treated as completely mixed in both scenarios.

The mass transfer model used to evaluate the ammonia release is the same as that used by Peurrung et al. (1998) to model ammonia evaporation from quiescent liquid in double-contained receiver tanks (DCRTs). (See Sections 2.5.1 and 2.5.1.2 of that reference for details.) Generally speaking, the model assumes that the liquid-side mass transfer coefficient for the slowly convecting liquid can be calculated from penetration theory, and the gas-side mass transfer coefficient is based on an analogy to the heat-transfer coefficient for free convection over a heated plate. The mass transfer rate is directly proportional to the area of the release (the whole tank area), the mass

(a) The back-dilution for crust sinking is somewhat higher here because the ammonia model assumes the slurry is fully mixed while the buoyancy/dissolution model does not mix below the injection point and applies an additional stratification factor.

Table 5.1. Waste Conditions for the Two Pool Evaporation Scenarios

	Initial Condition	Scenario 1	Scenario 2
Transferred waste (kgal)	0	300	300
Top-dilution water added (kgal)	0	78	265
Bottom-dilution water added (kgal)	0	35	35
Surface area exposed (%)	0	100	100
Waste surface elevation (in.)	431	332	399
Headspace volume (ft ³)		66,000	42,000
Top of mixed slurry (in.)	310	332	399
Crust NH ₃ dissolved concentration in liquid (M)	0.427	---	---
Slurry NH ₃ dissolved concentration in liquid (M)	0.214	0.218	0.172
Slurry avg. pressure (atm)	2.01	1.63	1.71
Temperature (C)	50.5	50.5	50.5

transfer coefficient, and the concentration driving force (which is the difference between the equilibrium ammonia vapor pressure and the partial pressure of ammonia in the headspace).

A liquid convection velocity of 0.03 m/s (110 m/hr) is assumed; this gives a liquid-side mass transfer coefficient of 2.8×10^{-6} (mol/m² s)/(Δmol/m³) for ammonia. This velocity implies that liquid crosses the tank from the center to the wall in six minutes, which is almost certainly an upper limit on velocity. The average convective velocity in the waste would be on the order of 1 m/hr to maintain a temperature difference of 0.1K with the undiluted heat generation rate of 44,000 Btu/hr.

The temperature difference driving headspace gas convection is assumed to be 1K, which is used to calculate a headspace gas convective velocity of 0.39 m/s. This gives a gas-side mass transfer coefficient of 1.5×10^{-3} (mol/m² s)/(Δmol/m³). The headspace gas would traverse the tank in one minute, consistent with the observed rapid headspace mixing. (For comparison, the modeled ventilation rate of 475 cfm would correspond to a gas velocity of roughly 0.005 m/s across the liquid surface.) Both of the mass-transfer coefficients are of the same order of magnitude as they were for the DCRT modeling, and as in that case the liquid-side mass transfer is limiting. The very approximate assumptions on which the mass-transfer coefficients are based leads to a large uncertainty, which was quantified with a simple sensitivity analysis, as discussed later.

The ammonia vapor pressure was calculated with the same version of the Schumpe gas solubility model that was used in DCRT modeling and in the RGS analysis (Peurrung et al. 1998, Mahoney et al. 1999). As noted in Section 3.6.1 of the latter reference, the Schumpe model can overestimate the vapor pressure of ammonia in concentrated salt solutions (that is, underestimate the solubility). The model has therefore been used (in the manner described in the reference) to

provide lower and upper bounds for the vapor pressure for ammonia release modeling. The effect of this uncertainty will be described later, as will the effect of the uncertainty in the mass transfer coefficients.

Details of the parameters used in the mass transfer model are given in Table 5.2. The headspace concentration was calculated by assuming dynamic equilibrium: that is, that the rate at which ammonia was carried out of the headspace by ventilation was equal to the rate at which it was evaporating from the surface. The dynamic concentration c and the time constant τ for the concentration rise transient are expressed as

$$c = \frac{c^*}{1 + E/kA} \quad (5.1)$$

$$\tau = \frac{V}{E + kA} \quad (5.2)$$

where

- c = dynamic equilibrium NH_3 concentration in domespace
- τ = time constant for the transient (time required for the concentration to rise 63% of the way to the final value c)
- c^* = domespace NH_3 concentration corresponding to vapor pressure
- E = volumetric ventilation rate
- K = overall mass-transfer coefficient for NH_3
- A = exposed liquid surface area
- V = domespace volume

Table 5.2. Mass Transfer Parameters for the Two Scenarios

	Scenario 1	Scenario 2
Ventilation rate (CFM)	475	475
Headspace temperature difference (K)	1	1
Gas-side mass-transfer coeff. for NH_3 ($\text{mol}/\text{m}^2 \text{ s}$) / ($\Delta\text{mol}/\text{m}^3$)	1.5×10^{-3}	1.5×10^{-3}
Waste liquid convection velocity (m/s)	0.03	0.03
Liquid-side mass transfer coeff. for NH_3 ($\text{mol}/\text{m}^2 \text{ s}$) / ($\Delta\text{mol}/\text{m}^3$)	2.8×10^{-6}	2.8×10^{-6}
Overall mass-transfer coefficient for NH_3 ($\text{mol}/\text{m}^2 \text{ s}$) / ($\Delta\text{mol}/\text{m}^3$)	9.3×10^{-5}	1.2×10^{-4}
Upper-bound ammonia vapor pressure (atm)	0.138	0.084
Lower-bound ammonia solubility ($(\text{mol}/\text{L waste}) / \text{atm}$)	1.4	1.9
Lower-bound ammonia vapor pressure (atm)	0.045	0.034
Upper-bound ammonia solubility ($(\text{mol}/\text{L waste}) / \text{atm}$)	4.3	4.8

At the modeled ventilation rate of 475 cfm and the headspace volumes corresponding to the waste levels for the two scenarios, the ammonia concentration will require about an hour to reach the dynamic equilibrium concentrations (assuming constant domespace volume, mass transfer coefficients, and area).

5.2 Predicted Ammonia Concentrations

Table 5.3 shows the headspace ammonia concentrations that were calculated for the two scenarios using the mass-transfer coefficients and the ammonia vapor pressures in Table 5.2. Scenario 1 (78-kgal dilution after a 300-kgal transfer) produces the higher concentration of the two scenarios. Although the ammonia vapor pressure varies by a factor of about 3 over the range from upper to lower bound, the headspace ammonia only varies by a factor of about 40% because the concentration is limited by the mass transfer rate. For comparison, the equilibrium state for the upper-bound vapor pressure for Scenario 1 would have produced an ammonia concentration of 135,000 ppm. Mass transfer significantly limits the ammonia concentration in the headspace.

The uncertainty in the convective velocities that determine the mass transfer coefficients must also be considered. The ammonia concentration is not sensitive to headspace convection, as determined from the headspace temperature difference. The concentration changes only 5%, from 19,000 ppm to 20,000 ppm, with an order of magnitude change in headspace temperature difference from 0.3 to 3K. It is more sensitive to the liquid convective velocity. Decreasing the liquid velocity an order of magnitude, from 110 m/hr to 11 m/hr, decreases the ammonia concentration about three-fold, from 15,000 to 6,000 for Scenario 2 as shown in Figure 5.1. This sensitivity was to be expected because the liquid-side mass-transfer is limiting.

Mahoney et al. (1999) suggest that (based on ammonia vapor pressure measurements over SY-101 simulants [Norton and Pederson 1994]) the best estimate for the vapor pressure at 50°C is about halfway between the lower and upper bounds. This implies that, for default mass transfer coefficients, the headspace concentration (at dynamic equilibrium) is about 17,000 ppm for Scenario 1 and 13,000 ppm for Scenario 2. Thus the conservatism in the upper-bound ammonia concentrations in Table 5.3 that is attributable to the vapor pressure model alone is less than 20%. Figure 5.2 shows the effect of solubility changes (vapor pressure changes) on the headspace ammonia for Scenario 2.

Table 5.3. Headspace Ammonia for Default Mass Transfer

	Scenario 1	Scenario 2
For upper-bound ammonia vapor pressure	20,000 ppm	15,000 ppm
For lower-bound ammonia vapor pressure	14,000 ppm	11,000 ppm

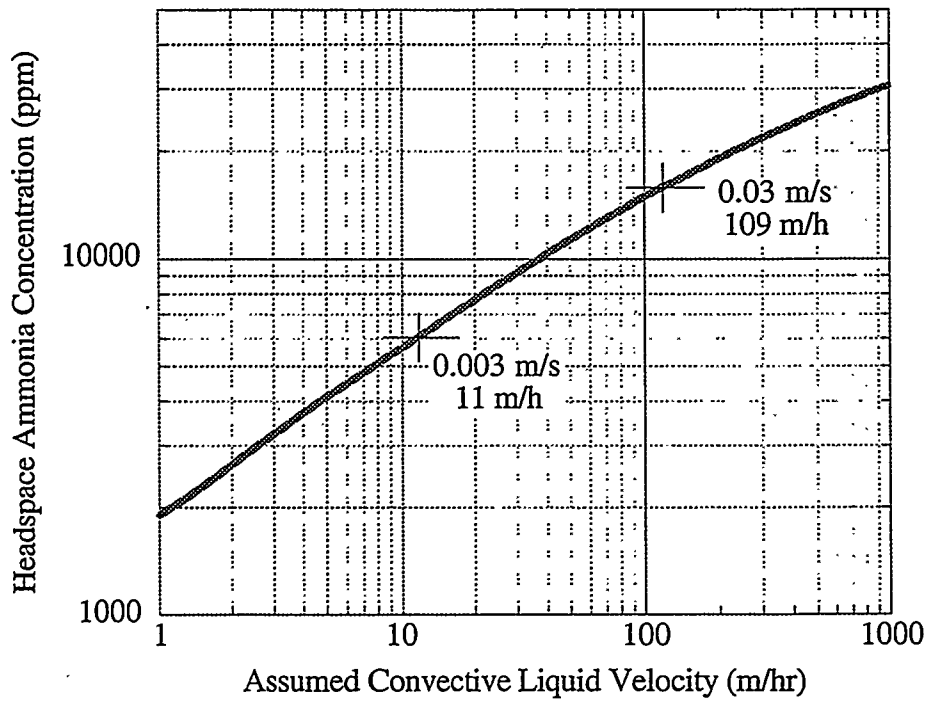


Figure 5.1. Headspace Ammonia Concentration versus Assumed Liquid Velocity

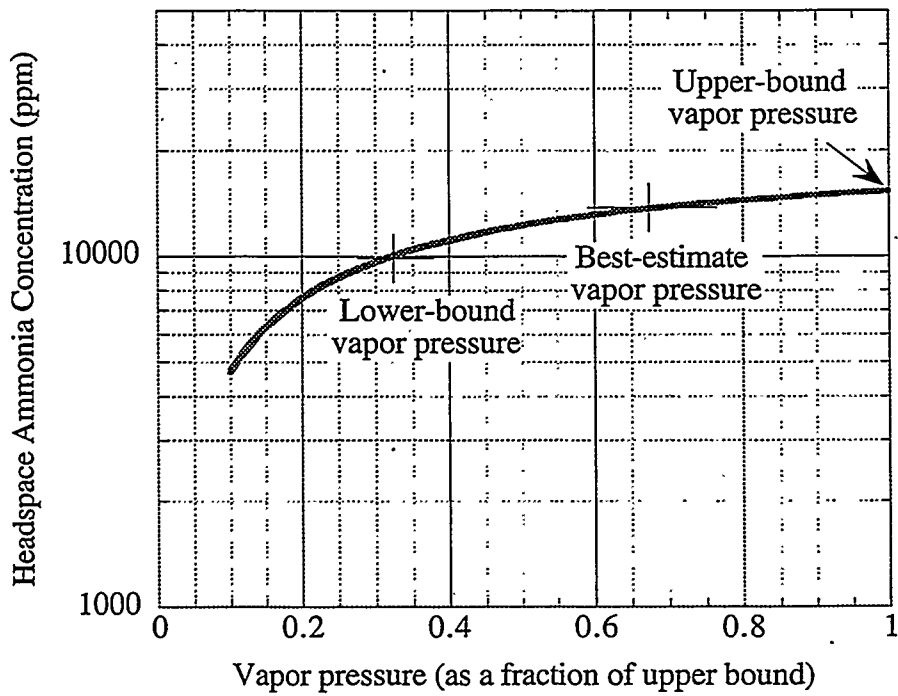


Figure 5.2. Headspace Ammonia Concentration versus Assumed Vapor Pressure

The assumption that the entire liquid surface will be exposed is another conservatism and is the upper limit. The headspace NH_3 concentration is nearly linearly proportional to the exposed area. If only half the area were exposed, the headspace concentrations shown in Table 5.3 would be reduced by a factor of 2, and so on. Figure 5.3 shows this linear dependence.

On the whole, the concentrations of 17,000 ppm (Scenario 1) and 13,000 ppm (Scenario 2) are probably very conservative estimates (primarily because of the liquid convective velocity and surface area assumptions) and may not be credible. (Even so, note that these concentrations are an order of magnitude less than the LFL for ammonia of 15% [150,000 ppm].)

The increased ammonia concentrations would be expected to persist as long as the liquid remained exposed. However, a thin, foamy carbonate crust is expected to form after the crust dissolves that will limit the ammonia evaporation to approximately current background levels. Also, the liquid surface will not suddenly appear to cause a sudden step to the high ammonia concentrations. As stated in Section 4, the crust is not expected to sink at all but to dissolve into islands and "bergs" that would slowly allow ammonia evaporation to increase. At the same time, the thin foam would fill in between the remaining crust as it dissolves to keep ammonia concentrations low.

The headspace ammonia concentration would be reduced to 3000 to 4000 ppm for the two scenarios if 1) only half of the tank area is exposed liquid (equivalent to a central pool with an 8.1-m (26-ft.) radius), 2) the convective liquid velocity is reduced to 11 m/hr (33 ft/hr), which is an order of magnitude less than the assumed value but still an order of magnitude more than the average velocity estimated to keep the liquid temperature uniform, and 3) an ammonia vapor

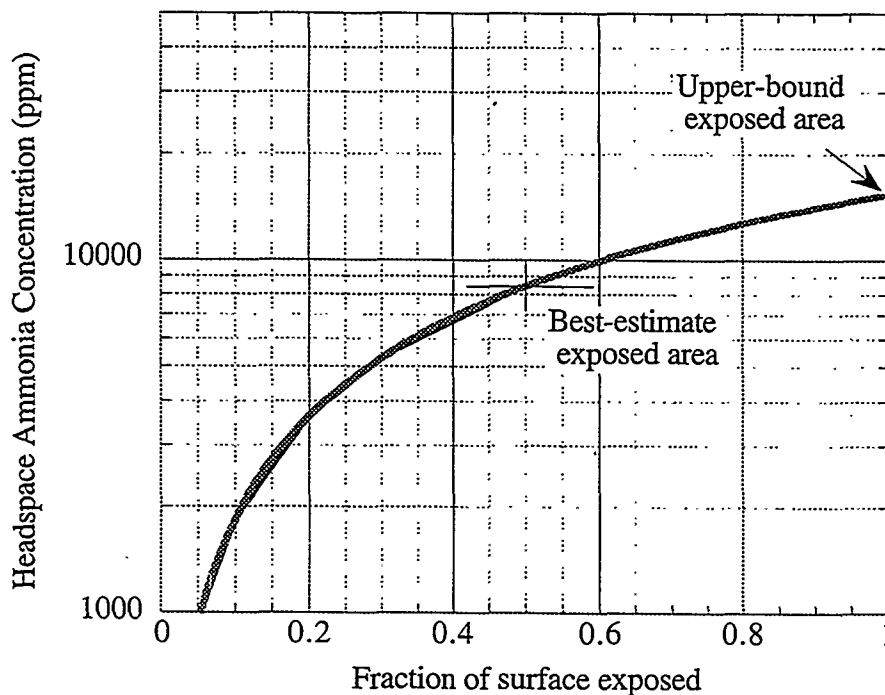


Figure 5.3. Headspace Ammonia Concentration versus Assumed Area

pressure midway between the upper and lower bounds is used. This concentration of 3000 to 4000 ppm is considered to be a best estimate. Note that the peak ammonia concentration in SY-102 at the end of the first transfer of waste from SY-101 was almost 2000 ppm and still rising. Though this may have been due to bubble entrainment by the downcomer siphon break in SY-102, it does emphasize the potential effect of the higher ammonia concentration in SY-101 waste.

If the SY-101 headspace ammonia concentration begins to rise too high, a simple mitigating action is additional top dilution water. Not only has the top dilution shown to be an effective scrubber of ammonia already in the headspace, the lighter water will float on top of the heavier brine to form an effective (though not permanent) barrier to further ammonia evaporation.

We conclude that, though high headspace ammonia concentrations can be expected in SY-101 when liquid is exposed, it should require on the order of an hour to build up. Should high ammonia concentrations become a problem, effective mitigation methods are available.

6.0 Summary and Conclusions

Four hazardous conditions created by crust sinking or dissolution were considered in this report: gas release by general bubble slurry flow through a thinned crust, gas retention due to crust encroachment on the mixer pump inlet, gas retention due to the inability of the mixer pump to mobilize a sunken crust, and ammonia evaporation from a free surface. The conclusions from analyses of both the flammability and toxicological hazards are provided below.

6.1 Flammability Hazard of Bubble Slurry Flow

A bubble slurry release cannot create a flammable headspace under current or foreseeable conditions. When the crust is predicted to sink, the surface level will be about 330 inches. The current bubble slurry layer contains 80 scm of gas. If the postulated instantaneous bubble slurry release occurs during sinking, the headspace hydrogen concentration would be about 1.6%, or 45% of the LFL.

If sinking does not occur, the paste layer is predicted to be fully dissolved after another 15 kgal of top back-dilution, which would raise the surface level to about 335 inches. The release of the entire bubble slurry layer at this level would raise the headspace hydrogen concentration to 1.65%, 47% of the LFL. In either case, the thickness of the bubble slurry layer could double and the gas release would still not exceed the LFL. Potential flammability due to a bubble slurry flow is thus dismissed as a hazard.

6.2 Ammonia Releases from Bubble Slurry Flow

Elevated ammonia concentrations are expected during and after a bubble slurry flow due to evaporation from the wet, newly exposed surface. (Mahoney et al. 1999). The headspace concentration is estimated by scaling up the ammonia release from a recently observed bubble slurry flow event to match the entire bubble slurry volume. During the January 7 flow event, a minimum of 0.89 scm (31 scf) of gas was released into this headspace to raise the hydrogen concentration from 67 to 384 ppm (see Figure 2.2). This is 1/90 of the 80 scm contained in the 10-inch bubble slurry layer. The corresponding ammonia release during the flow event was 0.11 scm (3.9 scf). Multiplying this release volume by the scale-up factor of 90 yields an estimate of 10 scm (356 scf) for the ammonia release from the entire bubble slurry layer.

Assuming a waste level at sinking of 330 inches, the 10 scm of ammonia would result in an ammonia concentration of 5,300 ppm. Because small bubble slurry flows are apparently occurring regularly and because the existing and expected nonuniformity of crust thickness will prevent a sudden, complete release, this is very much a bounding value for bubble slurry flow.

6.3 Crust Encroachment on the Mixer Pump Inlet

If the crust begins sinking, it will accelerate as the increasing hydrostatic pressure compresses the retained gas. The crust can stop descending short of the tank bottom only if it encounters fluid

that is dense enough to float the compressed material. A high-density layer that could support a sunken crust can potentially exist only just below the injection elevation.

For the planned low back-dilution, the injection point is the base of the transfer pump at 96 inches. At this elevation, the crust would need to be 140 inches thick just to reach the main inlet. Since the crust was never more than 120 inches thick and is predicted to be only 64 inches thick when it sinks, we conclude that crust encroachment into the mixer pump by sinking cannot occur with low back-dilution.

If the crust sinks during top dilution, its thickness will be half what it would be by low dilution, but the interface between the high- and low-density fluid will be only slightly above the main inlet after the second transfer. If the bubble slurry did not release its gas on sinking as expected, the crust could theoretically stop descending at this level. This would not necessarily affect the mixer pump at all. However, if necessary, low back-dilution would raise the crust base to whatever level might be required to clear the inlet.

The hypothetical possibility that a segment of crust could “hang up” on the pump column around the inlet after waste level is lowered by the transfer is also discounted based on the behavior of the crust during the first campaign.

6.4 Inability to Mobilize Sunken Crust

The result of crust sinking onto the 50-inch loosely settled layer due to low back-dilution is a nonconvective layer 114 inches thick immediately after sinking. We assume the sunken crust has the maximum yield strength computed for the paste layer of 3000 Pa. Under these conditions, it can be mobilized to a radius of just over 4 meters. This leaves over 87% of the sunken crust unmobilized. If a BD GRE occurred after the third campaign, about 340 scm of gas would be released, which would bring the headspace hydrogen concentration to over 12%, over three times the LFL. If the third campaign is not performed, the GRE would result in a headspace hydrogen concentration of 7%, exactly twice the LFL. Assuming one-fourth of the sunken crust could become buoyant at one time, in view of the nonuniformity of the current crust, results in a hydrogen concentration just over 3%, or 88% of the LFL after the third campaign. One-fourth of the gas release under post-second campaign conditions would produce 50% of the LFL.

Allowing the crust strength to weaken to 600 Pa and eliminating the 50-inch loosely settled layer from the BD GRE would roughly double the margin to the LFL would reduce the worst case consequence to 65% of the LFL. It is more likely that the sunken crust would largely dissolve after the third campaign or be eroded away by repeated pump runs. The crust is actually not expected to sink at all but break up the crust into small segments instead. For all these reasons we believe that, despite the results of the very conservative analysis, crust sinking by low dilution will not actually create conditions that would degrade the mixer pump’s ability to mitigate gas retention. The possibility of a sunken crust experiencing a large BD GRE is extremely remote.

When dissolved from the top down, the crust thickness is only 30 inches, 10 inches of which is the bubble slurry layer, which is assumed to disintegrate during sinking. With the 50-inch loosely settled layer, the resulting nonconvective layer is 70 inches thick immediately after sinking. The sunken crust is also assumed to have a yield stress from 600 Pa. Under these conditions, the

sunken crust can be mobilized to a radius of over 9 meters, leaving only 32% unmobilized. The result of a BD GRE from this material after the third campaign would raise the hydrogen concentration to just under 3%, 78% of the LFL. If we allow only one-fourth of the sunken crust to participate, as in the previous case, the resulting hydrogen concentration is only 0.7%, or 20% of the LFL. For post-second campaign conditions, the maximum instantaneous release would reach less than 50% of the LFL.

Based on the above evaluation and noting again the long list of conservative assumptions required to create the scenario (see Section 4.1), BD GREs engendered by a sunken crust are dismissed as a hazard. However, top back-dilution is recommended because it results in the least potential for gas retention.

6.5 Ammonia Evaporation from an Open Pool

When the crust dissolves, an exposed liquid pool might form that would allow ammonia to evaporate into the headspace at a rapid rate. This release could continue indefinitely unless it was retarded by a new crust or foam forming over the exposed liquid. The worst case analyzed is that a liquid pool forms when the crust sinks after a 78-kgal (total) dilution following a 300-kgal (total) transfer. Mass transfer significantly limits the ammonia concentration in the headspace. The worst-case (and probably incredible) headspace concentration is about 17,000 ppm.

Actually, a foamy "scum" of crust fragments and new carbonate crust is expected to form that will severely limit ammonia evaporation. When best estimates are used for the surface area exposed (50%) and the convective liquid velocity (which controls the mass transfer coefficient), the peak ammonia concentration is reduced to 4,000 ppm.

If the SY-101 headspace ammonia concentration begins to rise too high, a simple mitigating action is additional top-dilution water. Not only has top dilution shown to be an effective scrubber of ammonia already in the headspace, the lighter water floats on top of the heavier brine to form an effective, if temporary, barrier to further evaporation.

6.6 Overall Conclusion

A large transfer and back-dilution that effectively eliminates the current crust layer can be performed safely. While it is possible to create conditions that would exceed the LFL or produce high concentrations of ammonia in very specific hypothetical situations, we believe the list of improbably conservative assumptions required to make them happen is long enough to make them incredible.

7.0 References

Mahoney LA, ZI Antoniak, JM Bates, and ME Dahl. 1999. *Retained Gas Sampling Results for the Flammable Gas Program*. PNNL-13000, Pacific Northwest National Laboratory, Richland, Washington.

Meyer PA, ME Brewster, SA Bryan, G Chen, LR Pederson, CW Stewart, and G Terrones. 1997. *Gas Retention and Release Behavior in Hanford Double-Shell Waste Tanks*. PNNL-11536 Rev. 1, Pacific Northwest National Laboratory, Richland, Washington.

Peurrung LM, LA Mahoney, CW Stewart, PA Gauglitz, LR Pederson, SA Bryan, and CL Shepard. 1998. *Flammable Gas Issues in Double-Contained Receiver Tanks*. PNNL-11836 Rev. 1, Pacific Northwest National Laboratory, Richland, Washington.

Rassat SD, BE Wells, CW Stewart, JM Cuta, WL Kuhn, ZI Antoniak, KP Recknagle, G Terrones, JH Sukamto, VV Viswanathan, DP Mendoza. 2000. *Dynamics of Crust and Gas Release in Tank 241-SY-101*. PNNL-13112, Pacific Northwest National Laboratory, Richland, Washington.

Slezak SE, DC Williams, W Cheng, F Gelbard and DR Bratzel. 1998. *Refined Safety Analysis Methodology for Flammable Gas Risk Assessment in the Hanford Site Tanks*. HNF-SD-WM-ES-410 Rev. 2, Fluor Daniel Hanford, Inc., Richland, Washington.

Stewart CW, JM Alzheimer, G Chen, and PA Meyer. 1998. *In Situ Void Fraction and Gas Volume in Hanford Tank 241-SY-101 as Measured with the Void Fraction Instrument*. PNNL-12033, Pacific Northwest National Laboratory, Richland, Washington.

Distribution

<u>No. of Copies</u>		<u>No. of Copies</u>	
Offsite			
	WL Kubic		SD Estey R2-11
	Los Alamos National Laboratory		JM Grigsby R1-44
	PO Box 1663 K575		CE Hanson S7-70
	Los Alamos, NM 87545		GD Johnson (3) S7-73
			NW Kirch R2-11
			LJ Kripps S7-73
			CE Leach R1-44
			RE Raymond S7-70
Onsite			DA Reynolds R2-11
8	<u>DOE Richland Operations Office</u>	30	<u>Pacific Northwest National Laboratory</u>
	CA Groendyke (6)	H6-60	ZI Antoniak K7-15
	DH Irby	H6-60	JM Bates K7-15
	JS Shuen	H6-60	SQ Bennett K7-90
			JW Brothers (3) K9-20
18	<u>PHMC Team</u>		JM Cuta K7-15
	WB Barton	R2-11	PA Gauglitz K6-28
	RE Bauer	S7-73	JL Huckaby K7-15
	JR Biggs	S7-07	WL Kuhn K7-15
	C Carro	R1-44	LA Mahoney (3) K7-15
	RJ Cash	S7-73	DP Mendoza S3-32
	A-MF Choho	R3-73	PA Meyer K7-15
	JM Conner	R2-11	SD Rassat K6-28
			CW Stewart (5) K7-15
			JH Sukamto K8-93
			G Terrones K7-15
			BE Wells K7-15
			VV Viswanathan K6-28
			Information Release (5) K1-06